Internal Injection into the NRL Modified Betatron*

F. Mako, J. Golden, L. Floyd, K. McDonald, T.Smith,
and C. A. Kapetanakos
Plasma Physics Division, Naval Research laboratory,
Washington, D. C. 20375

Summary

We are reporting preliminary experimental results on the injection and trapping in the NRL Modified Betatron. In internal injection, the beam is produced by a diode located within the chamber. Using one half of the 1 m toroidal vacuum chamber, the propagated beam current and displacement are monitored as functions of the applied magnetic fields (B_z, and the toroidal field, B_θ). Our preliminary results are in agreement with theoretical predictions.

Introduction

The modified betatron accelerator (MBA) employs a toroidal magnetic field in addition to the conventional betatron field.[1,2] Theoretical analyses have shown that B_θ improves the equilibrium and stability properties and makes possible high circulating currents.[3,4] The space charge limiting current in the MBA is much higher than in a conventional betatron. The maximum equilibrium current of electrons with energy ~1 MeV in a torus having a major radius, $r_o \approx 1$ m is $\simeq 2.2$ kA when $B_\theta \sim 1$ kG.

Because of the higher current that can be confined as a result of B_θ, the self fields of the beam produce image forces and a hoop stress that alter the value of B_z that is needed to maintain the beam on an orbit at the injection radius, R. The required B_z is given by:

$$B_z = B_z^{sp}\left[1+\frac{2\nu}{\gamma}\left[1/2+\ln\frac{a}{r_b}+\frac{R(R-r_o)}{a^2(\gamma\beta)^2}+\frac{r_b^2}{8a^2(\gamma\beta)^2}\right]\right], \quad (1)$$

where B_z^{sp} is the single particle field = $m_o c\gamma\beta/(eR)$, ν is the Budker parameter, γ is the relativistic factor, β is the velocity divided by the speed of light, a is the chamber minor radius, r_b is the beam minor radius, m_o is the rest mass of the electron, and e is the electron charge.[5] For a 1 MeV, 1 kA beam, $\nu/\gamma \simeq 0.02$ and the B_z is about 10% higher than B_z^{sp}.

The applied B_θ introduces a poloidal drift motion of the beam that makes injection more complicated. Therefore, the transverse dynamics have been subject to extensive analytic and numerical study.[5,6] The drift surfaces have been computed from the constants of the motion and compared to simulation. The image forces contribute to the poloidal drift motion of the beam centroid. However, when $\nu/\gamma \ll 1$, and the beam is not very near the wall, the contribution of the image forces to the drift can be neglected. It is possible to exactly balance the forces on the beam so that the beam does not drift poloidally. In that case, the beam would strike the back of the cathode from which it was emitted after one revolution. However if B_z is mismatched from the value specified by eqn.(1), a poloidal drift that is initially predominantly either upwards or downwards will occur for a beam initially injected on the midplane of the device. The direction of the drift depends on whether B_z is too high or too low compared to the matched B_z value. When the space charge can be neglected, the initial drift velocity is given by

$$\dot{z} = v_\theta \frac{B_z}{B_\theta}\left\{\frac{\delta B_z}{B_z}\right\}, \quad (2)$$

where δB_z is the deviation from the matched value B_z given by eqn. 1 when space charge effects are neglected, B_θ is the toroidal field at the injection radius, and v_θ is the azimuthal electron velocity.

For successful internal injection, the poloidal drift must be fast enough so that the beam will miss the injector diode after one revolution. The beam must also be a a drift surface that avoids contact with the chamber wall. After a poloidal oscillation, the beam will then return to the injection point. The poloidal oscillation period is on the order of 1/4 microsec. This is sufficient time to slightly change the local B_z and shift the equilibrium position of the beam away from the injector. Such a change can be accomplished by a set of pulsed coils located inside the vacuum chamber.[7]

The present paper reports the experimental results of beam propagation around one half of the torus. The beam is observed to successfully propagate to a Faraday collector. The dependence of the poloidal drift on γ and B_z is studied, and the effect of B_θ on transport is determined.

Experimental Set-up

The NRL Modified Betatron comprises air-cored, pulsed electromagnet coils that produce the applied betatron (BF) and toroidal (TF) magnetic fields, a structure to hold the coils in position, a toroidal vacuum chamber, and an injector accelerator.[8,9] A schematic plan view of the accelerator is shown in Fig. 1.

The coils are powered by capacitor bank discharge. In the present studies, the fields are "crowbarred" just after the peak field. Risetimes are 1.6 msec (BF) and 1.7 msec (TF). The BF and TF waveforms are reproducible to within 1%. The TF coils are a set of 12 single turn rectangular coils connected in series. The BF coils consist of 18 single turn hoops that are connected in series. There are also 5 single turn trimmer coils that can be used to adjust B_z and n in the vicinity of the chamber. At R=1.09 m, $n \sim .6$-$.7$.

The vacuum chamber torus major radius is 1.00 m and the minor radius is 15.3 cm. The chamber consists of 30° sectors and is evacuated to base pressures of 3×10^{-6} Torr. The chamber wall is 0.45 mm thick stainless steel overwrapped with epoxy-fiberglas reinforcement. The magnetic diffusion time of the chamber is 0.35 microsec.

The injector consists of a Marx generator/pulse forming transmission line and a beam-producing diode.[10] Nominal injection parameters are energy 1 MeV, current 1-2 kA, and pulse duration 20-40 nsec (flattop). The electrons are injected along the B_θ at R = 1.09 m. The injector shot-to-shot variation of peak voltage applied to the diode (V_d) is 0.9 %. A typical waveform of V_d is shown in Fig. 2.

The diode consists of a 0.7 cm radius carbon cathode, spaced 1.5 cm from the anode (see Fig. 3). In the present experiment, the anode is a 75% transparent screen of 0.5 mm diam. stainless steel wire. Surrounding the anode screen is a carbon annulus that provides field shaping and intercepts unwanted electrons emitted by the cathode stalk. The anode is supported by a 2 cm ID, 5 cm long stainless steel tube that is electrically connected to the torus.

Diagnostic measurements are made of the diode voltage by a resistive divider at the output insulator of the injector pulse generator and by a capacitive divider located at the injection port of the torus. The currents flowing through the cathode stalk and through the anode support are also monitored. Beam current(I_{FC}) is monitored by a Faraday collector(FC) that can be placed at various azimuthal positions around the torus. The FC consists of a 9 cm diam. beam target and a single turn Rogowski coil to measure the collected current flowing to the torus. The FC is mounted on an acrylic end plate that blanks off the torus. A grounded stainless steel foil backed by x-ray intensifier film is placed in front of the end plate and behind the beam target. Open shutter photography of the beam produced x-rays provides information about the time-integrated poloidal position and spot size of the beam.

Experimental Results

The beam current is measured at 10°,70°, and 130° from the injection point. With V_d=750 kV, I_{FC}=750-800 A at 10°. At 70°, I_{FC}=720 A, and at 130°, I_{FC}=640 A. The dependence of I_{FC} with B_z is plotted in Fig. 4. A broad peak is obtained at 70° because the FC target is large and the propagation distance is short so that even poorly matched beams do not have time to drift sufficiently to miss the FC. As expected, the curve becomes narrower at 130°. because ,for a given B_z, the beam has more time to drift before reaching the azimuthal position of the FC.

Measurement of beam current at 130°. for γ= 2.0, 2.5, and 3.05 as a function of B_z is shown in Fig. 5. The peak currents increase with γ because the injected current is larger for a diode impedance that is matched to the pulse generator. The value of B_z corresponding to the peak I_{FC} for different γ is plotted in Fig. 6 and compared with the prediction of eqn. (1).

As B_θ is varied, the beam spot size becomes smaller. For an injected 1 MeV, 1 kA beam, I_{FC}=600 A when B_θ=1.0 kG, and the beam spot size is larger than the FC target. However, for the same injection conditions, I_{FC}=1.0 kA when B_θ=1.5 kG and the spot size is 2-3 cm diam.

A poloidal displacement of the beam spot is observed as a result of the drift motion. As shown in Fig. 7, this displacement can be sufficient to miss the FC target completely at 130°. According to eqn. (2), the intial drift of the beam centroid is a function of γ which varies in time during the pulse. Thus, the time-integrated beam spot is spread out because of the time variation of V_d. Consequently, the shape of I_{FC} should vary as a function of B_z for a given V_d. This is shown in Fig. 8 by representative traces of I_{FC} for three different B_z. In the top trace, the lower energy electrons in the rising and falling portion of the injected pulse miss the FC. In the middle trace, the entire pulse is collected and the waveform has the same shape as the injected diode current. In the bottom trace, only the rising and falling portions of the pulse are collected.

* Supported by ONR and SDIO.

References

[1] P. Sprangle and C. A. Kapetanakos, J. Appl. Phys. 49 1 (1978).

[2] H. Ishizuka, G. Lindley, B. Mandelbaum, A. Fisher and N. Rostoker, Phys. Rev. Lett. 53 266 (1984).

[3] C. A. Kapetanakos, P. Sprangle, D. Chernin, S. J. Marsh, and I. Haber, Phys. Fl. 26 1634 (1983).

[4] P. Sprangle and J. Vomvoridis, Memo. Rept.4688, NRL, Washington, D.C.(1982).

[5] C. A. Kapetanakos and S. J. Marsh, Memo. Rept. 5387, NRL, Washington, D.C. (1984).

[6] C. Agritellis, S. J. Marsh, and C. A. Kapetanakos, Part. Accel. 16 155 (1985).

[7] C. A. Kapetanakos, P. Sprangle, and S. J. Marsh, Phys. Rev. Lett. 49 741 (1982).

[8] J. Golden, J. Pasour, D. E. Pershing, K. Smith, F. Mako, S. Slinker, F. Mora, N. Orrick, R. Altes, A. Fliflet, P. Champney, and C. A. Kapetanakos, IEEE Trans. Nuc. Sci. NS-30 2114 (1983).

[9] F. Mako, K. Smith, J. A. Pasour, K. McDonald, R. Altes, J. Golden, and C. A. Kapetanakos, Proc. IEEE 10th Symp. on Fusion Eng., Philadelphia PA, 5-9 Dec 1983, 705 (1984).

[10] Beta Development Corp., Dublin, CA.

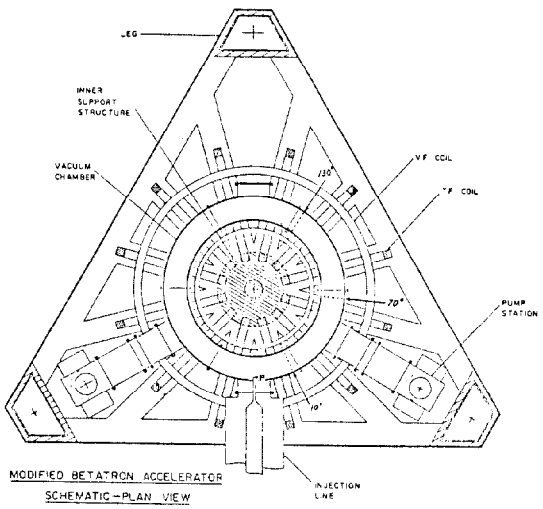

Fig.1. MODIFIED BETATRON ACCELERATOR SCHEMATIC-PLAN VIEW

Fig. 2. Typical V_d waveform, vert. 267 kV/div, horiz. 20 nsec/div.

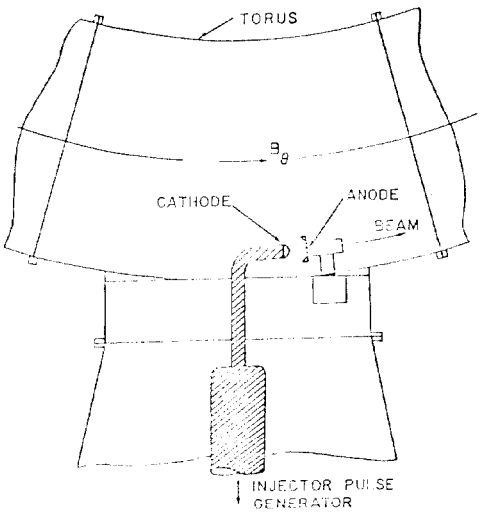

Fig. 3. Schematic of internal injection.

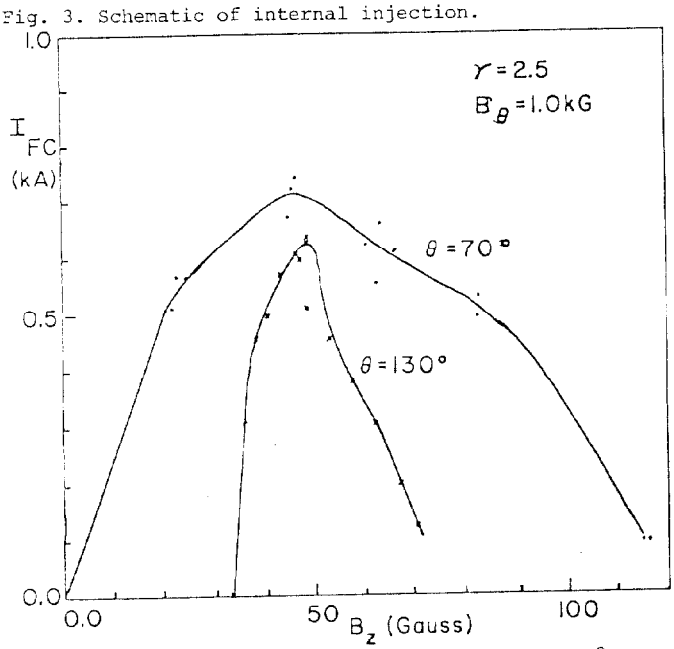

Fig. 4. Current at Faraday collector vs. B_z and θ.

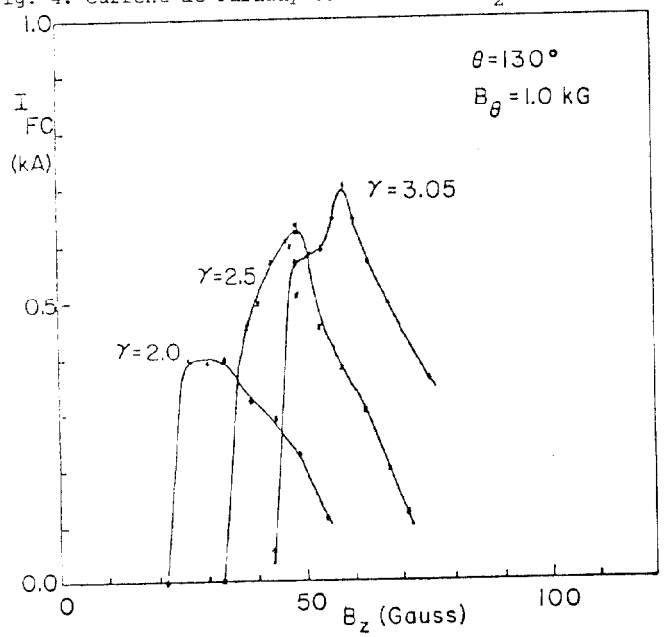

Fig. 5. Current at Faraday collector vs. B_z and γ.

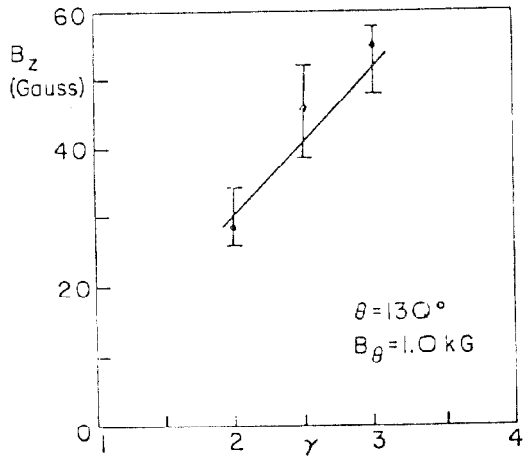

Fig. 6. B_z for peak propagated current vs. γ.

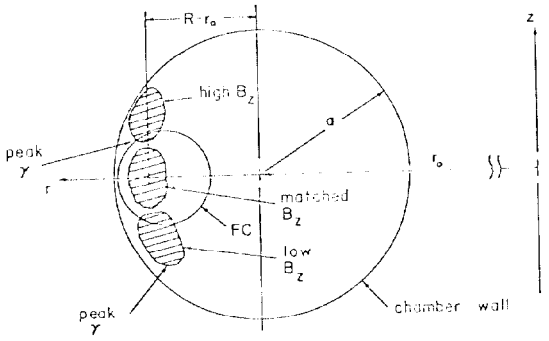

Fig. 7. Minor cross section of torus at the Faraday collector azimuth showing position of beam spot at high, matched, and low B_z.

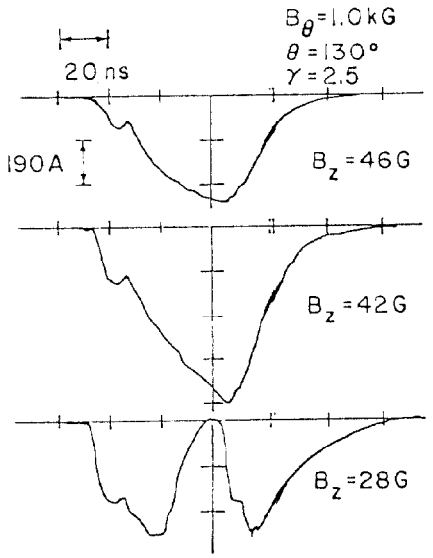

Fig. 8. Representative I_{FC} traces as B_z varies.